

Bayesian Nonparametric Inference in Elliptic PDEs: Convergence Rates and Implementation

Matteo Giordano¹

¹University of Turin, Corso Unione Sovietica 218 bis, Turin, Italy

Abstract

Parameter identification problems in partial differential equations (PDEs) consist in determining one or more functional coefficient in a PDE. In this article, the Bayesian nonparametric approach to such problems is considered. Focusing on the representative example of inferring the diffusivity function in an elliptic PDE from noisy observations of the PDE solution, the performance of Bayesian procedures based on Gaussian process priors is investigated. Building on recent developments in the literature, we derive novel asymptotic theoretical guarantees that establish posterior consistency and convergence rates for methodologically attractive Gaussian series priors based on the Dirichlet–Laplacian eigenbasis. An implementation of the associated posterior-based inference is provided and illustrated via a numerical simulation study, where excellent agreement with the theory is obtained.

Keywords. inverse problems; Gaussian priors; frequentist consistency; posterior mean; Markov chain Monte Carlo

1 Introduction

Partial differential equations (PDEs) are primary mathematical tools to model the behaviour of complex real-world phenomena, with ubiquitous applications across engineering and the sciences. The formulation of a PDE typically involves a number of *functional parameters*, which are often unknown in applications and not directly accessible to measurements. Employing a PDE model in practice therefore necessitates that the parameters in the equation be determined beforehand from the available data, giving rise to an *inverse problem of parameter identification*. Such problems have been extensively studied in applied mathematics [1, 2, 3] and, more recently, in statistics [4, 5, 6]. See the monographs [7, 8, 9] and the references therein for an extended overview on this research area.

In the present paper, we shall focus on the following representative example. Consider a physical quantity undergoing *diffusion* in an inhomogeneous multidimensional convex medium $\mathcal{O} \subset \mathbb{R}^d$, $d \in \mathbb{N}$, with smooth boundary $\partial\mathcal{O}$. At equilibrium, the density $u(x)$ of the diffusing substance at any location $x \in \mathcal{O}$ is governed by the second-order elliptic PDE

$$\begin{cases} \nabla \cdot (f \nabla u) = s, & \text{on } \mathcal{O} \\ u = b, & \text{on } \partial\mathcal{O}, \end{cases} \quad (1)$$

where $s : \mathcal{O} \rightarrow \mathbb{R}$ describes the spatial distribution of local sources or sinks, $g : \partial\mathcal{O} \rightarrow \mathbb{R}$ prescribes the density values at the boundary, and the *diffusivity function* $f : \mathcal{O} \rightarrow (0, \infty)$

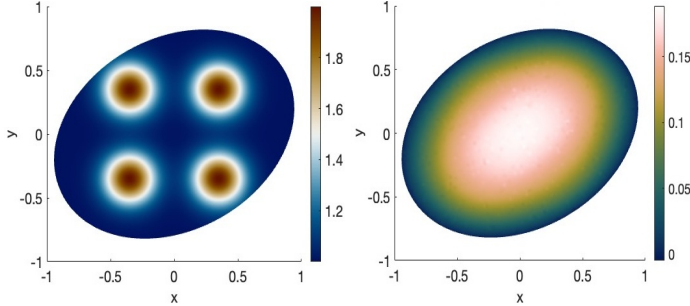


Figure 1: **(Left):** An example of diffusivity function f with four circular regions of higher conductivity. **(Right):** $n = 4500$ noisy observations from the corresponding PDE solution $G(f)$.

models spatially varying conductivity throughout the inhomogeneous domain. Under mild regularity conditions on the PDE coefficients, standard elliptic theory implies the existence of a unique twice continuously differentiable classical solution $G(f) \equiv u_f \in C^2(\mathcal{O})$ to (1) (e.g., [10], Chapter 6). Assuming that s and b are known, we are then interested in the problem of estimating f from n noisy point evaluations of $G(f)$ over a grid of (possibly random) design points X_1, \dots, X_n in \mathcal{O} ,

$$Y_i = G(f)(X_i) + \sigma W_i, \quad i = 1, \dots, n, \quad (2)$$

where W_1, \dots, W_n are statistical measurement errors, and $\sigma > 0$ is the noise level. In view of the central limit theorem, the Gaussian assumption $W_1, \dots, W_n \stackrel{\text{iid}}{\sim} N(0, 1)$ can often be realistically maintained. The inverse problem of recovering the diffusivity in the elliptic PDE (1) from observations of its solution is an important building block in oil reservoir modelling [11], where u is the (accessible to measurements) fluid pressure, and f is the (not directly observable) permeability field, which can exhibit drastic spatial variations due to changes in the reservoir composition. This problem has been studied in a large number of articles in applied mathematics, e.g., [12, 13, 14], and statistics, e.g., [5, 15, 16]. An illustration on a bi-dimensional domain is given in Figure 1.

While the PDE (1) is linear, the parameter-to-solution map $f \mapsto G(f)$ is not, which poses several methodological and theoretical challenges. In particular, least squares functionals involving $G(f)$ are generally non-convex so that commonly used optimisation-based methods (such as Tikhonov regularisation, maximum likelihood or maximum-a posteriori estimation) cannot reliably be implemented by standard convex optimisation techniques. In this context, the Bayesian approach to inverse problems, popularised by influential work by Stuart [17], offers an attractive alternative. In the Bayesian framework, the unknown parameter f is regarded as a random variable (with values in a function space) and assigned a *prior probability distribution* $\Pi(\cdot)$ that models the available information about f before collecting the observations. The prior is then combined, through *Bayes' formula*, with the data $\{(Y_i, X_i)\}_{i=1}^n$ to form the *posterior distribution* $\Pi(\cdot | \{(Y_i, X_i)\}_{i=1}^n)$, which represents the updated belief about f and is used to draw the inferences. As the posterior formally involves only evaluations of the prior and the likelihood (cf. Equation (7) below), the approximate computation of $\Pi_n(\cdot | \{(Y_i, X_i)\}_{i=1}^n)$ and its associated *posterior mean estimator* $\hat{f}_n := E^\Pi[f | \{(Y_i, X_i)\}_{i=1}^n]$ via sampling methods is feasible as long as the forward map G can be numerically evaluated. For the elliptic PDE (1), this can be performed using

efficient PDE solvers based on finite element methods, sidestepping altogether the need for a (possibly non-existent) inversion formula for G , as well as the use of optimisation approaches. In particular, for the class of *Gaussian process priors*, efficient ad hoc Markov chain Monte Carlo (MCMC) algorithms, suited to the present infinite-dimensional setting, have been developed, e.g., [16]. A further decisive advantage of the Bayesian methodology is that, alongside point estimates, it also automatically delivers *uncertainty quantification* for the recovery via the spread of the posterior, used in applications to provide interval-type estimators and to construct hypothesis tests.

The success and popularity in applications has led to recent interest in the literature for the derivation of theoretical performance guarantees for nonparametric Bayesian procedures in PDE models [18, 19, 20, 21, 22, 23]. This is motivated by the fact that the performance of Bayesian methods depends on a suitable choice of the prior, which in infinite-dimensional statistical models primarily serves as a regularisation tool, and whose specification is a delicate task in its own right (cf. Section 1.2 in [24]). Thus, the question arises as to whether Bayesian procedures may provide valid and prior-independent inference, at least in the presence of informative data. The established paradigm under which such investigation is carried out is the *frequentist analysis* of Bayesian procedures, assuming that the observations are generated by a fixed *ground truth* f_0 and studying the concentration of the posterior towards f_0 in the large sample size limit. We refer the reader to [24] for an introduction to this research area.

The present paper is concerned with the performance of Bayesian nonparametric methods based on Gaussian priors in the elliptic inverse problem (2). In Section 2, we provide a general result that establishes posterior consistency and convergence rates of the conditional mean estimator for a general class of Gaussian priors (Theorem 1). We then apply our general theorem to obtain statistical recovery rates for truncated Gaussian series priors defined on the eigenbasis of the Dirichlet–Laplacian (Example 2), which is a commonly used basis of practical interest offering a convenient and generally applicable framework for implementation; cf. Section 3.1. This shows that the resulting procedures provide statistically valid estimation of the diffusivity f , with explicit estimation error bounds that decay algebraically in the number n of observations. Our results extend upon the recent investigation of Giordano and Nickl [20], who considered Gaussian priors associated to popular covariance kernels (such as the Matérn or squared-exponential ones), as well as truncated Gaussian wavelet series expansions but did not explore the methodologically attractive procedures based on the Dirichlet–Laplacian eigenbasis constructed herein.

Furthermore, in Section 3, we complement the theoretical results with a discussion on implementation, devising two different discretisation strategies. The first is tailored to applications where a specific set of basis functions is of interest. In particular, in Section 3.1, we employ the Dirichlet–Laplacian eigenbasis, discretising the parameter space by high-dimensional truncated series expansions in accordance with our theoretical results. In the second approach, described in Section 3.2, we discretise the parameter space via piecewise linear functions defined on the elements of a deterministic triangular mesh, which is naturally suited to implementing Gaussian priors specified via a covariance kernel. Here, the popular Matérn kernel is employed for illustration. A numerical simulation study is provided to investigate the performance of the inferential procedures under the two discretisation strategies. In our numerical experiments, both approaches yielded satisfactory results, comparable in terms of reconstruction quality and running time. The posterior mean estimate (relative to a Matérn process prior), computed via a Metropolis–Hastings-type MCMC algorithm, is shown in Figure 2 for increasing sample sizes, to be compared to

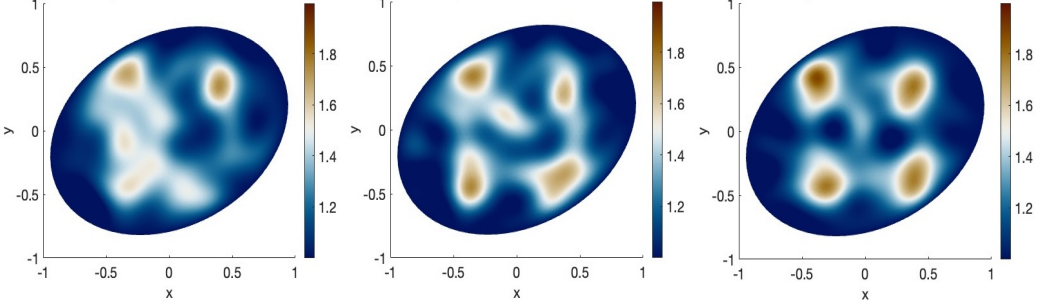


Figure 2: Left to right: posterior mean estimates \bar{f}_n of the diffusivity function f for increasing sample sizes $n = 100, 250, 1000$.

the true diffusion coefficient pictured in Figure 1 (left). The reproducible MATLAB code used for the study is available at <https://github.com/MattGiord> (accessed on 19 March 2025).

2 Materials and Methods

2.1 Likelihood, Prior and Posterior

Throughout, $\mathcal{O} \subset \mathbb{R}^d$, $d \in \mathbb{N}$, is a given nonempty, open, convex and bounded set with smooth boundary $\partial\mathcal{O}$. For the observation model (2), with $G(f)$ as the solution to the PDE (1), and for fixed constants $\alpha > 1 + d/2$ and $f_{\min} > 0$, we take the parameter space

$$\mathcal{F}_{\alpha, f_{\min}} := \left\{ f \in H^\alpha(\mathcal{O}) : \inf_{x \in \mathcal{O}} f(x) \geq f_{\min}, f|_{\partial\mathcal{O}} \equiv 1, \frac{\partial^j f}{\partial \nu^j} \equiv 0 \text{ for } 1 \leq j \leq \alpha - 1 \right\}, \quad (3)$$

with $H^\alpha(\mathcal{O})$ as the usual Sobolev space of regularity α and $\nu(x)$, $x \in \partial\mathcal{O}$, the unit normal vector. Assuming that the source term s in (1) is fixed and smooth, and taking (without loss of generality) homogeneous Dirichlet boundary conditions $b \equiv 0$, the Schauder theory for elliptic PDEs (e.g., Theorem 6.14 in [10]) implies that for each $f \in \mathcal{F}_{\alpha, f_{\min}}$, there exists a unique classical solution $G(f) \in C(\overline{\mathcal{O}}) \cap C^{1+\alpha}(\mathcal{O})$ to the elliptic PDE (1). We then assume data $\{(Y_i, X_i)\}_{i=1}^n$ arising as in Equation (2) for some unknown $f \in \mathcal{F}_{\alpha, f_{\min}}$, with independent and identically distributed (i.i.d.) random design variables X_1, \dots, X_n following the uniform distribution on \mathcal{O} . Throughout, we regard the noise level $\sigma > 0$ in (2) as fixed and known; in practice, it may often be replaced by an estimate (cf. Section 4). In view of the i.i.d. standard normal assumption on the noise variables W_1, \dots, W_n in (2), the random vectors $\{(Y_i, X_i)\}_{i=1}^n \sim P_f^{(n)}$ have joint probability density function in product form,

$$p_f^{(n)}(\{(x_i, y_i)\}_{i=1}^n) = \frac{1}{(2\pi\sigma^2)^{n/2}} e^{-\sum_{i=1}^n [y_i - G(f)(x_i)]^2 / (2\sigma^2)}, \quad y_i \in \mathbb{R}, \quad x_i \in \mathcal{O}.$$

Accordingly, the log-likelihood is seen to be equal to, up to an additive constant, the negative least-square functional

$$l_n(f) := -\frac{1}{2\sigma^2} \sum_{i=1}^n [Y_i - G(f)(X_i)]^2, \quad f \in \mathcal{F}_{\alpha, f_{\min}}. \quad (4)$$

In a recent paper by Giordano and Nickl [20], posterior consistency and convergence rates for the conditional mean estimator have been established for nonparametric Bayesian procedures based on Gaussian process priors. To incorporate the shape constraints in the parameter space $\mathcal{F}_{\alpha, f_{\min}}$, ref. [20] employed the parametrisation

$$f = \Phi \circ F, \quad (5)$$

where $F \in H_0^\alpha(\mathcal{O})$ (the completion of $C_c^\infty(\mathcal{O})$ with respect to $\|\cdot\|_{H^\alpha}$) and $\Phi : \mathbb{R} \rightarrow [f_{\min}, \infty)$ is a *regular link function*, that is a smooth, strictly increasing and bijective function with bounded derivatives and such that $\Phi(0) = 1$. An instance of regular link function is provided in Example 24 of [20]. In practice, the exponential link $\Phi(\cdot) = \exp(\cdot)$ is often used. In the following, we occasionally switch between the notation f and F , implicitly making use of the relation (5).

Under the parametrisation (5), placing a prior probability distribution $\Pi(\cdot)$ on F induces a (push-forward) prior on f , which, in slight abuse of the notation, we still denote by $\Pi(\cdot)$. Following [20], we consider *scaled* Gaussian priors, constructed starting from a base (possibly n -dependent) centred Gaussian Borel probability measure Π_{W_n} , which we assume to be supported on a measurable linear subspace of the Hölder space $C^\beta(\mathcal{O})$, for some $\beta \geq 1$, and to have reproducing kernel Hilbert space (RKHS) \mathcal{H}_{W_n} continuously embedded into $H_0^\alpha(\mathcal{O})$. See Chapter 2 in [25] for the background and terminology on Gaussian processes and measures. Given Π_{W_n} , we then construct the scaled prior $\Pi_n(\cdot)$ as the law of the random function

$$V(x) := \frac{W(x)}{n^{d/(4\alpha+4+2d)}}, \quad x \in \mathcal{O}, \quad W \sim \Pi_{W_n}(\cdot). \quad (6)$$

By linearity, $\Pi_n(\cdot)$ also defines a centred Gaussian Borel probability measure with the same support as Π_{W_n} ; the scaling enforces the additional regularisation used in the theoretical analysis to deal with the nonlinearity of the inverse problem.

Given prior $\Pi_n(\cdot)$ as above, by Bayes' formula (p. 7, [24]), the posterior distribution $\Pi_n(\cdot | \{(Y_i, X_i)\}_{i=1}^n)$ of $F | \{(Y_i, X_i)\}_{i=1}^n$ arising from data in model (2) equals

$$\Pi_n(B | \{(Y_i, X_i)\}_{i=1}^n) = \frac{\int_B e^{l_n(\Phi \circ F)} d\Pi_n(F)}{\int_{C(\mathcal{O})} e^{l_n(\Phi \circ F')} d\Pi_n(F')}, \quad B \subseteq C(\mathcal{O}) \text{ measurable}, \quad (7)$$

with $l_n(\cdot)$ as the log-likelihood in (4).

2.2 Convergence Rates

We study the asymptotic concentration of the posterior distribution $\Pi_n(\cdot | \{(Y_i, X_i)\}_{i=1}^n)$ in (7) around the ground truth diffusivity function $f_0 = \Phi \circ F_0$, assuming that the data $\{(Y_i, X_i)\}_{i=1}^n \sim P_{f_0}^{(n)}$ have been generated according to the observation model (2) with $f = f_0$. The following theorem extends the main result of [20], allowing to include in

the analysis general sieve-type Gaussian priors, cf. Example 2. The proof follows through similarly to Section 3.2 in [20]; it is included for completeness and the convenience of the reader in Appendix B.

Theorem 1. *For fixed positive integers $\alpha, \beta \in \mathbb{N}$ such that $\alpha > \beta + d/2$, consider the scaled prior Π_n in (6), where Π_{W_n} is a centred Gaussian Borel probability measure supported on a measurable linear subspace of $C^\beta(\mathcal{O})$, with RKHS $\mathcal{H}_{W_n} \subseteq H_0^\alpha(\mathcal{O})$ satisfying, for some constant $c > 0$ (independent of n),*

$$\|F\|_{H^\alpha} \leq c\|F\|_{\mathcal{H}_{W_n}}, \quad \forall F \in \mathcal{H}_{W_n}.$$

Further assume that

$$\sup_{n \in \mathbb{N}} E^{\Pi_{W_n}} \|F\|_{C^1} < \infty.$$

For fixed $F_0 \in H_0^\alpha(\mathcal{O})$, suppose that there exists a sequence $F_{0,n} \in \mathcal{H}_{W_n}$ such that, as $n \rightarrow \infty$,

$$\|F_0 - F_{0,n}\|_{(H^1)^*} = O(n^{-\frac{\alpha+1}{2\alpha+2+d}}); \quad \max\{\|F_{0,n}\|_{C^1}, \|F_{0,n}\|_{\mathcal{H}_{W_n}}\} = O(1). \quad (8)$$

Then, there exists $L > 0$ that is large enough such that, as $n \rightarrow \infty$,

$$\Pi_n \left(f : \|G(f) - G(f_0)\|_{L^2} > Ln^{-\frac{\alpha+1}{2\alpha+2+d}} \middle| \{(Y_i, X_i)\}_{i=1}^n \right) \rightarrow 0, \quad (9)$$

in $P_{f_0}^{(\infty)}$ -probability as $n \rightarrow \infty$. If in addition $\beta \geq 2$ and $\inf_{x \in \mathcal{O}} s(x) > 0$, then there exists $L > 0$ that is large enough and a constant $\lambda > 0$ such that

$$\Pi_n(f : \|f - f_0\|_{L^2} > Ln^{-\lambda} \mid \{(Y_i, X_i)\}_{i=1}^n) \rightarrow 0, \quad (10)$$

in $P_{f_0}^{(\infty)}$ -probability as $n \rightarrow \infty$, and moreover, the estimator $\bar{f}_n = \Phi \circ \bar{F}_n$, with $\bar{F}_n = E^{\Pi_n}[F \mid \{(Y_i, X_i)\}_{i=1}^n]$, satisfies as $n \rightarrow \infty$,

$$P_{f_0}^{(n)}(\|\bar{f}_n - f_0\|_{L^2} > n^{-\lambda}) \rightarrow 0. \quad (11)$$

The first statement (Equation (9)) of Theorem 1 establishes posterior consistency in *prediction risk*: The induced posterior on the PDE solution $G(f)$, $f \sim \Pi_n(\cdot \mid \{(Y_i, X_i)\}_{i=1}^n)$, concentrates around the true PDE solution $G(f_0)$ in L^2 -distance at rate $n^{-(\alpha+1)/(2\alpha+2+d)}$. Since such a rate is known to be minimax optimal [26] (Theorem 10), procedures satisfying the assumption of Theorem 1 are seen to optimally solve the PDE-constrained regression problem of recovering $G(f_0)$ from data $\{(Y_i, X_i)\}_{i=1}^n$.

The second statement shows that the posterior contracts around f_0 also in the standard L^2 -risk, thereby solving the inverse problem of estimating the diffusivity. It follows combining (9) with the regularisation properties implied by the rescaling in the prior construction (6) and a suitable *stability estimate* for G^{-1} . The latter was proved in [26] (Lemma 24), and requires the slightly stronger assumption on β and the strict positivity of the source s . The exponent $\lambda > 0$ is explicitly computed in the proof of Theorem 1 and equals $\lambda = (\alpha + 1)(\beta - 1)/(2\alpha + 2 + d)(\beta + 1)$. Note that $\lambda < (\alpha + 1)/(2\alpha + 2 + d)$. While minimax optimal rates for estimating the diffusivity f in model (2) are currently unknown, inspection of the proof shows that when $f_0 \in C^\infty(\mathcal{O})$, then the prior can be tuned so to attain a rate as closed as desired to the parametric rate $n^{-1/2}$.

The last statement of Theorem 1 entails that the estimator \bar{f}_n converges towards f_0 in L^2 -risk at the same rate $n^{-\lambda}$ attained by the whole posterior distribution. It is indeed a corollary of (10), following from uniform integrability arguments for Gaussian measures and the Lipschitzianity of the composition with the link function Φ .

2.3 Examples of Gaussian Priors

We now provide two concrete instances of Gaussian priors to which Theorem 1 applies. For both examples, an implementation of the associated posterior-based inference is provided in Section 3 below. We maintain the assumption that $f_0 = \Phi \circ F_0$ for some $F_0 \in H^\alpha(\mathcal{O})$ supported inside a given compact subset $K \subset \mathcal{O}$. This corresponds to the common assumption that f_0 is known near the boundary $\partial\mathcal{O}$ (specifically $f_0 \equiv 1$ on $\mathcal{O} \setminus K$).

We first consider high-dimensional Gaussian sieve priors obtained via truncating Karhunen–Loëve-type random series expansions, a frequently used approach in computation, e.g., [27]. In particular, via Theorem 1, we study procedures based on the Dirichlet–Laplacian eigenbasis. Such constructions corresponds to commonly used Gaussian process priors with covariance kernel given by an inverse power of the Laplacian, e.g., [17] (Section 2.4). The eigenbasis can be numerically computed via efficient finite element methods for elliptic eigenvalue problems, offering a broadly applicable framework for implementation on general domains \mathcal{O} . Details on computation and a numerical simulation study are provided in Section 3.1.

Example 2 (Dirichlet–Laplacian eigenbasis). *Let $\{e_j, j \geq 0\} \subset H_0^1(\mathcal{O}) \cap C^\infty(\overline{\mathcal{O}})$ be the orthonormal basis of $L^2(\mathcal{O})$ formed by the eigenfunctions of the (negative) Dirichlet–Laplacian:*

$$\begin{cases} -\Delta e_j - \lambda_j e_j = 0, & \text{on } \mathcal{O} \\ e_j = 0, & \text{on } \partial\mathcal{O}, \end{cases} \quad j \geq 0, \quad (12)$$

with associated eigenvalues $0 < \lambda_0 < \lambda_1 \leq \lambda_2 \leq \dots$, satisfying $\lambda_j \rightarrow \infty$ as $j \rightarrow \infty$ according to Weyl's asymptotics: $\lambda_j = O(j^{2/d})$ as $j \rightarrow \infty$, cf. Figures 3 and 4. See Example 6.3 and Section 7.4 in [28] for details. Define the Hilbert scale

$$\mathbb{H}^s := \left\{ w \in L^2(\mathcal{O}) : \|w\|_{\mathbb{H}^s}^2 := \sum_{j=0}^{\infty} \lambda_j^s |\langle w, e_j \rangle_2|^2 < \infty \right\}, \quad s \geq 0.$$

We then have $\mathbb{H}^0 = L^2(\mathcal{O})$ (with equality of norms), $\mathbb{H}^1 = H_0^1(\mathcal{O})$ (with equivalence of norms), $\mathbb{H}^2 = H_0^1(\mathcal{O}) \cap H^2(\mathcal{O})$, and the continuous embedding $\mathbb{H}^s \subset H^s(\mathcal{O})$ for all $s \geq 0$ (holding generally with strict inclusion), cf. p. 472f. in [29]. In fact, it holds that $\|w\|_{\mathbb{H}^s} \simeq \|w\|_{H^s}$ for all $w \in \mathbb{H}^s$ and $s \geq 0$ (proved initially for $s = 2$, then extended by induction to all larger integers, and finally by interpolation to all positive reals), and if $F \in H^s(\mathcal{O})$ is compactly supported within \mathcal{O} , then $F \in \mathbb{H}^s$. Finally, defining $\mathbb{H}^{-1} := (\mathbb{H}^1)^ = (H_0^1(\mathcal{O}))^*$, we have the equivalence (cf. Equation (A15) in [29])*

$$\|w\|_{(H_0^1)^*}^2 \simeq \|w\|_{\mathbb{H}^{-1}}^2 := \sum_{j=0}^{\infty} \lambda_j^{-1} |\langle w, e_j \rangle_2|^2. \quad (13)$$

Now for fixed $J \in \mathbb{N}$, the Gaussian random sum

$$\bar{W}_J := \sum_{j \leq J} \lambda_j^{-\alpha/2} W_j e_j, \quad W_j \stackrel{\text{iid}}{\sim} N(0, 1),$$

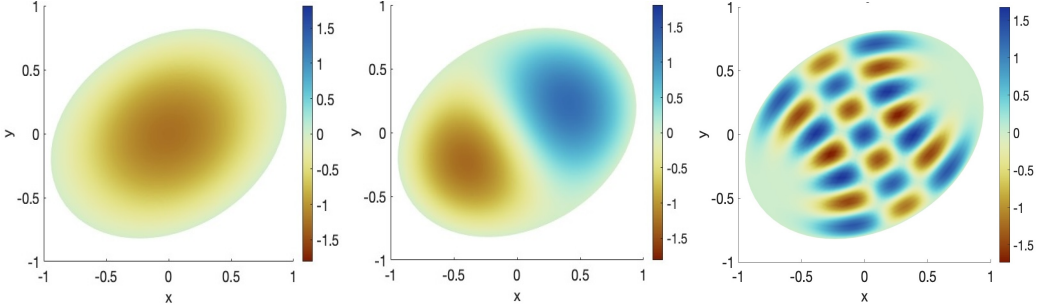


Figure 3: Left to right: The first, second, and fiftieth Dirichlet–Laplacian eigenfunctions e_0 , e_1 and e_{49} , computed via finite element methods.

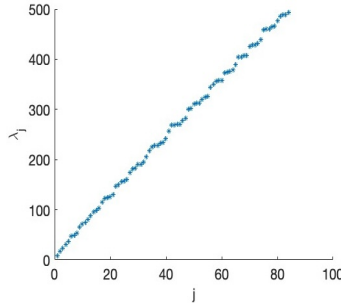


Figure 4: Dirichlet–Laplacian eigenvalues λ_j in the range $[0, 500]$, computed via finite element methods.

defines a centred Gaussian Borel probability measure supported on (and with RKHS equal to) the finite-dimensional space $\mathcal{H}_{\overline{W}_J} := \text{span}\{e_j, j \leq J\}$, with RKHS norm

$$\|\bar{w}\|_{\mathcal{H}_{\overline{W}_J}}^2 = \sum_{j \leq J} \lambda_j^\alpha w_j^2 = \|\bar{w}\|_{\mathbb{H}^\alpha}^2 \simeq \|\bar{w}\|_{H^\alpha}^2, \quad \forall w \in \overline{W}_J.$$

Fix any smooth cut-off function $\chi \in C_c^\infty(\mathcal{O})$ such that $\chi = 1$ on K , and consider the random function

$$W_n := \chi W_{J_n} = \sum_{j \leq J_n} \lambda_j^{-\alpha/2} W_j \chi e_j, \quad W_j \stackrel{\text{iid}}{\sim} N(0, 1), \quad (14)$$

where $J_n \in \mathbb{N}$ is such that $J_n \simeq n^{d/(2\alpha+2+d)}$. By the linearity and boundedness of multiplication by χ , the law Π_{W_n} of W_n defines, according to Exercise 2.6.5 in [25], a centred Gaussian prior supported on (and with RKHS equal to)

$$\mathcal{H}_{W_n} = \text{span}\{\chi e_j, j \leq J_n\} \subset C_c^\infty(\mathcal{O}) \subset \bigcap_{s=0}^{\infty} H_0^s(\mathcal{O}) \cap \bigcap_{s=0}^{\infty} \mathbb{H}^s,$$

with RKHS norm satisfying, with a multiplicative constant independent of n ,

$$\|\chi \bar{w}\|_{\mathcal{H}_{W_n}} \leq \|\bar{w}\|_{\mathcal{H}_{\overline{W}_{J_n}}} \simeq \|\bar{w}\|_{H^\alpha}, \quad \forall \bar{w} \in \mathcal{H}_{\overline{W}_{J_n}}.$$

Arguing as in Example 25 in [20], one further shows that for some constant $c > 0$ (inde-

pendent of n),

$$\|w\|_{H^\alpha} \leq c\|w\|_{\mathcal{H}_{W_n}}, \quad \forall w \in \mathcal{H}_{W_n}.$$

Finally, by a Sobolev embedding and the above inequality,

$$E^{\Pi_{W_n}} \|F\|_{C^1}^2 \lesssim E^{\Pi_{W_n}} \|F\|_{H^\alpha}^2 \leq c E^{\Pi_{W_n}} \|F\|_{\mathcal{H}_{W_n}}^2 \leq E \left[\sum_{j \leq J_n} \lambda_j^{-\alpha} W_j^2 \right],$$

which is uniformly bounded in n recalling that $W_i \stackrel{\text{iid}}{\sim} N(0, 1)$ and the fact that by Weyl's asymptotics $\lambda_j^{-\alpha} = O(j^{-2\alpha/d})$ with $\alpha > 1 + d/2$. This shows that the sequence of base priors Π_{W_n} satisfies the first two assumptions of Theorem 1. For ground truths $F_0 \in H^\alpha(\mathcal{O})$ compactly supported inside K , we have $F_0 \in \mathbb{H}^\alpha$. Construct the finite-dimensional approximations

$$F_{0,n} = \sum_{j \leq J_n} \langle F_0, e_j \rangle_2 \chi e_j \in \mathcal{H}_{W_n}, \quad n \in \mathbb{N}. \quad (15)$$

Then for all $n \in \mathbb{N}$,

$$\|F_{0,n}\|_{\mathcal{H}_{W_n}} \leq \left\| \sum_{j \leq J_n} \langle F_0, e_j \rangle_2 e_j \right\|_{\mathcal{H}_{W_{J_n}}} = \left\| \sum_{j \leq J_n} \langle F_0, e_j \rangle_2 e_j \right\|_{\mathbb{H}^\alpha} \leq \|F_0\|_{\mathbb{H}^\alpha} \simeq \|F_0\|_{H^\alpha} < \infty.$$

By a Sobolev embedding, we similarly have $\|F_{0,n}\|_{C^1} \leq \|F_0\|_{H^\alpha} < \infty$ for all $n \in \mathbb{N}$. Furthermore, since both F_0 and $F_{0,n}$ have compact support within \mathcal{O} ,

$$\begin{aligned} \|F_0 - F_{0,n}\|_{(H^1)^*} &= \sup_{H \in H^1(\mathcal{O})} \int_{\mathcal{O}} (F_0(x) - F_{0,n}(x)) H(x) dx \\ &= \sup_{H \in H_0^1(\mathcal{O})} \int_{\mathcal{O}} (F_0(x) - F_{0,n}(x)) H(x) dx = \|F_0 - F_{0,n}\|_{(H_0^1)^*}, \end{aligned}$$

and recalling (13), Weyl's asymptotics, and the choice of J_n ,

$$\begin{aligned} \|F_0 - F_{0,n}\|_{(H^1)^*}^2 &= \sum_{j > J_n} \lambda_j^{-(1+\alpha)} \lambda_j^\alpha |\langle F_0, e_j \rangle_2|^2 \\ &\leq \lambda_{J_n}^{-(1+\alpha)} \|F_0\|_{\mathbb{H}^\alpha}^2 \lesssim (J_n)^{-2(1+\alpha)/d} \simeq n^{-2(\alpha+1)/(2\alpha+2+d)}. \end{aligned}$$

We conclude that Theorem 1 applies with the sequence of base Gaussian sieve priors in (14), choosing the approximations $F_{0,n}$ according to (15).

The second main example, already considered in [20], concerns stationary Gaussian processes specified via a translation invariant covariance kernel. For concreteness, we focus on the popular Matérn kernel. Implementation of the resulting procedures is illustrated in Section 3.2.

Example 3 (Matérn covariance kernel). Consider a Matérn process $W = \{W(x), x \in \mathcal{O}\}$ on \mathcal{O} with regularity $\alpha - d/2$, that is a centred stationary Gaussian process with covariance

kernel

$$C(x, y) = \frac{2^{1-\alpha}}{\Gamma(\alpha)} \left(\frac{|x - y| \sqrt{2\alpha}}{\ell} \right)^\alpha B_\alpha \left(\frac{|x - y| \sqrt{2\alpha}}{\ell} \right), \quad x, y \in \mathcal{O}, \quad \ell > 0, \quad (16)$$

where Γ denotes the gamma function and B_α is the modified Bessel function of the second kind. Fix any smooth cut-off function $\chi \in C_c^\infty(\mathcal{O})$ such that $\chi = 1$ on K . It can then be shown (cf. Example 25 in [20]) that the law Π_W of χW defines a centred Gaussian Borel probability measure supported on the separable linear subspace $C^{\beta'}(\mathcal{O})$ of $C^\beta(\mathcal{O})$ for any $\beta < \beta' < \alpha - d/2$. Furthermore, its RKHS is given by $\mathcal{H}_W = \{\chi F, F \in H^\alpha(\mathcal{O})\} \subset H_0^\alpha(\mathcal{O})$, with the RKHS norm satisfying

$$\|\chi F\|_{H^\alpha} \lesssim \|\chi F\|_{\mathcal{H}_W}, \quad \forall F \in H^\alpha(\mathcal{O}).$$

For ground truths $F_0 \in H^\alpha(\mathcal{O})$ compactly supported inside K , we have $\chi F = F$, so that $F \in \mathcal{H}_W$. We conclude that Theorem 1 applies for a base Matérn process prior $\Pi_{W_n} := \Pi_W$, choosing the trivial approximating sequence $F_{0,n} := F_0$ for all $n \in \mathbb{N}$.

3 Results

We investigate the performance of the procedures based on the Gaussian priors considered in Examples 2 and 3 in a numerical simulation study. For illustration, we fix the working domain \mathcal{O} to the area contained inside the rotated ellipse, with $\theta = \pi/6$,

$$\partial\mathcal{O} = \{(\cos(t) \cos(\theta) - 0.75 \sin(t) \sin(\theta), 0.75 \sin(t) \cos(\theta) + \cos(t) \sin(\theta)), t \in [0, 2\pi)\},$$

and take the ground truth conductivity

$$f_0(x, y) = \sum_{k, m \in \{-1, 1\}} e^{-(5x+1.75k)^2 - (5y+1.75m)^2}, \quad (x, y) \in \mathcal{O}, \quad (17)$$

cf. Figure 1 (left). We then generate observations $\{(Y_i, X_i)\}_{i=1}^n$ according to (2). The true PDE solution $G(f_0)$ is numerically computed via finite element methods, using the MATLAB PDE Toolbox. For the experiments, the source function is set to $s(x, y) = \exp(-(5x - 2.5)^2 - (5y)^2) + \exp(-(7.5x)^2 - (2.5y)^2) + \exp(-(5x + 2.5)^2 - (5y)^2)$, $(x, y) \in \mathcal{O}$, and the noise standard deviation to $\sigma = 0.0025$ (with corresponding signal-to-noise ratio $\|G(f_0)\|_{L^2}/\sigma = 68.50$). Further experiments, with differently shaped ground truths, are presented in Appendix A.

3.1 Results with Truncated Gaussian Series Priors

To implement the truncated Gaussian series priors from Example 2, we numerically compute the first $J_n \simeq n^{d/(2\alpha+2+d)}$ Dirichlet–Laplacian eigenpairs via finite element methods; see Figures 3 and 4. Identifying the functional parameter F in (5) with the vector of coefficients $\mathbf{F} := [F_1, \dots, F_{J_n}]$, where $F_j := \langle F, e_j \rangle_2$, the prior then corresponds to

$$\mathbf{F} \sim N(0, \Lambda_n), \quad \Lambda_n := n^{-d/(2\alpha+2+d)} \text{diag}(\lambda_1^{-\alpha}, \dots, \lambda_{J_n}^{-\alpha}) \in \mathbb{R}^{J_n, J_n}. \quad (18)$$

While the employed prior is Gaussian, the nonlinearity of the forward map $f \mapsto G(f)$

implies that the log-likelihood $l_n(f)$ in (4) depends nonlinearly on f . The resulting posterior distribution is therefore generally non-Gaussian and not available in closed form. We then resort to MCMC sampling via the pCN algorithm [16], which is a specific instance of the random-walk Metropolis–Hastings method for Gaussian priors that is known to be robust to the discretisation dimension. In the present setting, we employ the pCN algorithm to generate an \mathbb{R}^{J_n} -valued Markov chain $(\mathbf{F}_h)_{h \geq 1}$ with invariant measure equal to the posterior distribution, starting from an initialisation point \mathbf{F}_0 and then, for $h = 0, 1, 2, \dots$, repeating the following steps:

1. Draw a prior sample $\xi \sim N(0, \Lambda_n)$, where Λ_n is as in (18), and for $\delta > 0$ define the proposal $p := \sqrt{1 - 2\delta} \mathbf{F}_h + \sqrt{2\delta} \xi$;

2. Set

$$\mathbf{F}_{h+1} := \begin{cases} p, & \text{with probability } 1 \wedge e^{l(\Phi \circ p) - l(\Phi \circ \mathbf{F}_h)}, \\ \mathbf{F}_h, & \text{otherwise,} \end{cases}$$

where l is the log-likelihood function in (4).

For each iteration, step 2 requires the evaluation of the log-likelihood $l_n(\Phi \circ p)$, which in turn entails the numerical evaluation of the PDE solution $G(\Phi \circ p)$ at the design points X_1, \dots, X_n , cf. (4), which we perform via finite element methods. The prior samples $\xi \sim N(0, \Lambda_n)$ required in step 1 are straightforward to draw since Λ_n is diagonal.

The algorithm is terminated after H steps, returning approximate samples $\{\mathbf{F}_h, h = 0, \dots, H\}$ from the posterior distribution, where a first batch of iterates is typically discarded as the burn-in. Under a set of assumptions on the forward map that is compatible with the present setting, Hairer, Stuart, and Vollmer [30] derived dimension-free spectral gaps which imply rapid convergence of the pCN marginal laws towards the invariant measure. As a consequence, the posterior mean \bar{F}_n can reliably be numerically computed by the MCMC average

$$\bar{\mathbf{F}} := \frac{1}{H+1} \sum_{h=0}^H \mathbf{F}_h, \quad (19)$$

with non-asymptotic bounds for the numerical approximation error. Posterior credible sets can likewise be reliably computed by considering the empirical quantiles of the pCN samples.

Figure 2 shows the posterior mean estimates $\bar{f}_n = \Phi \circ \bar{\mathbf{F}}_n$ of the conductivity function f obtained for increasing sample sizes $n = 100, 250, 1000$. The corresponding L^2 estimation errors (and the associated relative errors) are reported in Table 1 (first and second row), displaying a progressive decay as expected from the theory developed in Section 2. Across the experiments, the prior regularity parameter α in Equation (18) is set to $\alpha = 3 = 2 + d/2$. The pCN algorithm is iterated $H = 25,000$ times, and the first 5000 samples are discarded as the burn-in. The step size is set to $\delta = 0.0025, 0.001, 0.0005, 0.00025$, tuned depending on the sample size to obtain a stabilisation of the acceptance rate around 30% after the burn-in; see Figure 5 (left). A pCN *cold-start* $\mathbf{F}_0 = 0$ is employed. Figure 5 (right) shows, for the experiment with $n = 1000$, the log-likelihood $l_n(\Phi \circ \vartheta_h)$ along the first 3000 pCN iterates (part of the burn-in phase), seen to rapidly increase towards, and then stabilise around, the log-likelihood $l_n(f_0)$ attained by the true diffusivity f_0 . The computation time per experiment is around 50 min on a 2020 M1 MacBook Pro 13 running MATLAB 2024b.

Table 1: L^2 -estimation errors and relative errors for the posterior mean estimates with increasing sample sizes.

n	100	250	500	1000
$\ \bar{f}_n - f_0\ _{L^2}$; series prior	0.2981	0.2232	0.2144	0.1581
$\ \bar{f}_n - f_0\ _2 / \ \bar{f}_0\ _{L^2}$; series prior	17.67%	12.23%	12.71%	9.36%
$\ \bar{f}_n - f_0\ _{L^2}$; Matérn prior	0.3289	0.2677	0.2033	0.1647
$\ \bar{f}_n - f_0\ _2 / \ \bar{f}_0\ _{L^2}$; Matérn prior	18.98%	15.86%	12.05%	9.76%

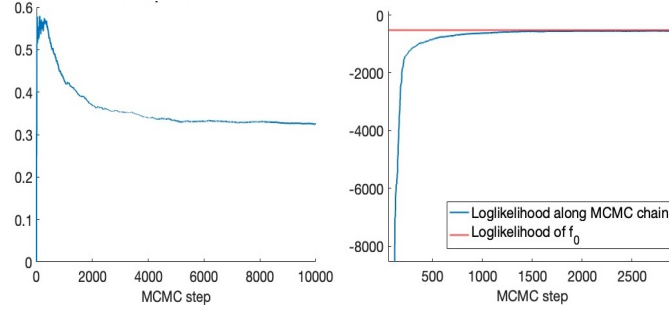


Figure 5: (Left): acceptance rate over the first 10,000 pCN samples. The rate stabilises around 30% after the initial burn-in time (first 5000 iterates). (Right): in blue, the log-likelihood $l_n(\Phi \circ \vartheta_h)$ of the first 3000 iterates; in red, the log-likelihood $l_n(f_0)$ of the true diffusion coefficient f_0 .

3.2 Results with the Matérn Process Prior

For Gaussian process priors specified via a covariance kernel, such as the Matérn process considered in Example 3, we discretise the parameter space by assuming that F in (5) is given by the finite sum

$$F = \sum_{m=1}^M F_m \psi_m, \quad F_m \in \mathbb{R}, \quad M \in \mathbb{N}, \quad (20)$$

where $\{\psi_1, \dots, \psi_M\}$ are piecewise linear functions on a deterministic triangular mesh with nodes $\{z_1, \dots, z_M\} \subset \mathcal{O}$, uniquely characterised by the relation $\psi_m(z_{m'}) = 1_{\{m=m'\}}$. Accordingly, F in (20) satisfies $F(z_m) = F_m$, and for any $x \in \mathcal{O}$, the value $F(x)$ is obtained by linear interpolation over the pairs $\{(z_m, F_m), m = 1, \dots, M\}$. Given the Matérn kernel C in (16), and identifying F with the vector of values $\mathbf{F} := [F_1, \dots, F_M]$, the prior then corresponds to

$$\mathbf{F} \sim N(0, \mathbf{C}), \quad \mathbf{C} = [C_{mm'}]_{m,m'=1}^M \in \mathbb{R}^{M,M}, \quad C_{mm'} = C(z_m, z'_m).$$

Posterior inference based on the Matérn process prior may be implemented via the pCN algorithm described in Section 3.1 above. For each iteration, the construction of the pCN proposal p in step 1 entails sampling an independent multivariate Gaussian random variable $\xi \sim N(0, \mathbf{C})$. In step 2, the computation of the acceptance probability requires the evaluation of the proposal log-likelihood $l_n(\Phi \circ p)$, which can be performed via numerical PDE methods as described above.

For the ground truth f_0 specified in Equation (17), Table 1 (third and fourth row) dis-

plays the L^2 -estimation errors (and the relative errors) associated to the posterior mean estimates $\bar{f}_n = \Phi \circ \bar{F}_n$ for increasing sample sizes $n = 100, 250, 500, 1000$. Across the experiments, the parameter space is discretised using a uniform triangular mesh with $M = 2000$ nodes. The hyperparameters for the Matérn covariance kernel in (16) are set to $\alpha = 3$ and $\ell = 0.25$. Similarly to the results in Section 3.1, the runs of pCN are stopped after $H = 25,000$ iterations, with a tuning of the step size (respectively, $\delta = 0.0025, 0.001, 0.0005, 0.00025$) to achieve a stabilisation of the acceptance rate at around 30% after the burn-in (corresponding to the first 5000 iterates). A non-informative initialisation point $\mathbf{F}_0 = 0$ is chosen for each run. The computation times ranges between 50 and 57 min, in line with those obtained for the truncated Gaussian series prior in Section 3.1.

4 Discussion

In this article, we have considered the nonparametric Bayesian approach to inference in elliptic PDEs, focusing on the standard benchmark problem of estimating the diffusivity function from noisy observation of the PDE solution. We have provided a general asymptotic concentration result, Theorem 1, for the posterior distribution and the posterior mean estimator, and showed that it applies to two classes of Gaussian priors of interest, namely truncated Gaussian series priors defined on the Dirichlet–Laplacian eigenbasis (cf. Example 2) and Matérn process priors (cf. Example 3). For both prior models, we have devised strategies for implementing the posterior-based inference, employing efficient and reliable MCMC algorithms. The performance of the considered methods has been investigated in a numerical simulation study, where excellent reconstruction results and a general agreement with the theory have been obtained. Overall, the main advantages of the approach lie in its modelling flexibility, and the robustness of the associated computational methods, as well as the availability of theoretical guarantees on the recovery performance.

Let us conclude overviewing some related research questions. Firstly, we remark that that the noise standard deviation σ in (2) is assumed to be known throughout the paper. In the realistic scenario where σ is also unknown, the methodology developed here can readily be adapted by replacing it (in an *empirical Bayes* spirit) with a preliminary (non-likelihood-based) estimate. Several strategies have been proposed in the literature for variance estimation in nonparametric regression models, ranging from residual-based estimators using kernel smoothing [31] and splines [32], to difference-based estimators [33]. Alternatively, a joint Bayesian model for f and σ in (2) could be considered by endowing σ with a prior distribution (for example, an independent conjugate inverse gamma prior). This leads to the interesting question concerning the extension of the theoretical results presented in Section 2 to the setting with unknown variance; see [34] for related results in a direct regression model.

Secondly, we mention the important issue of specifying the hyperparameter values for the considered prior distributions, namely, the regularity parameter α for the truncated Gaussian series prior from Example 2, and the smoothness and length-scale in the Matérn covariance kernel (16). There a vast literature investigating the methodological and theoretical aspects of empirical and hierarchical Bayesian strategies to fully data-driven hyperparameters selection; see [35, 36, 37, 38, 20], where many more references can be found. Investigating the implications and performance of these methods in the context of the elliptic PDE model and the Gaussian prior distributions considered in the present article is an interesting direction for future research.

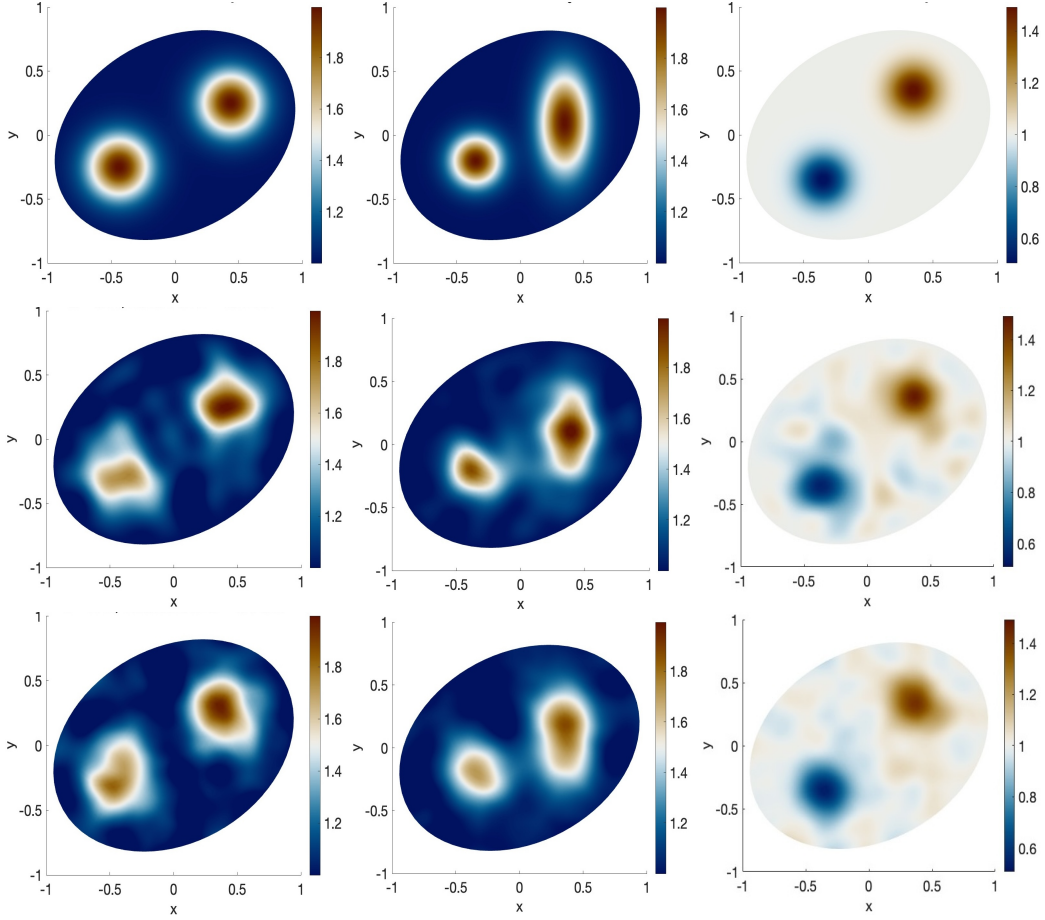


Figure 6: Left column, top to bottom, respectively: the ground truth corresponding to $F_0^{(1)}$, and the posterior mean estimates (computed via the pCN algorithm) for the truncated series and Matérn priors. The step size is set to $\delta = 0.00035, 0.0001$ respectively, and the acceptance ratios are 24.15% and 26.51%. Central column: the ground truth for $F_0^{(2)}$ and the posterior mean estimates. For pCN, $\delta = 0.0001, 0.00005$, acceptance ratios: 20.42% and 22.73%. Right column: the ground truth for $F_0^{(3)}$ and the posterior mean estimates. For pCN, $\delta = 0.0001, 0.000035$, acceptance ratios: 25.61%, 29.85%.

A Further Numerical Results

We present further empirical investigations in which we consider the recovery of three additional true diffusivity functions, respectively specified (under the parametrisation (5)) by

$$\begin{aligned}
 F_0^{(1)}(x, y) &= \log \left(1 + e^{-(4x-1.75)^2-(4y-1)^2} + e^{-(4x+1.75)^2-(4y+1)^2} \right); \\
 F_0^{(2)}(x, y) &= \log \left(1 + e^{-(5x-1.75)^2-(2.5y-0.25)^2} + e^{-(5x+1.75)^2-(5y+1)^2} \right); \\
 F_0^{(3)}(x, y) &= \log \left(1 + 0.5e^{-(5x-1.75)^2-(5y-1.75)^2} - 0.5e^{-(5x+1.75)^2-(5y+1.75)^2} \right),
 \end{aligned}$$

for $(x, y) \in \mathcal{O}$; see Figure 6, top row. For each ground truth, we generate synthetic datasets $\{(Y_i, X_i)\}_{i=1}^n$, with $n = 2500$ as described in Section 3, with noise standard deviation

Table 2: Recovery performances of the posterior mean estimate for different ground truths.

	$F_0^{(1)}$	$F_0^{(2)}$	$F_0^{(3)}$
$\ \bar{f}_n - f_0\ _{L^2}; \text{series prior}$	0.1197	0.0974	0.07234
$\ \bar{f}_n - f_0\ _{L^2}/\ f_0\ _{L^2}; \text{series prior}$	7.22%	5.90%	4.71%
$\ \bar{f}_n - f_0\ _{L^2}; \text{Matérn prior}$	0.1241	0.0941	0.08148
$\ \bar{f}_n - f_0\ _{L^2}/\ f_0\ _{L^2}; \text{Matérn prior}$	7.49%	5.70%	5.31%

$\sigma = 0.0025$ (and signal-to-noise ratio respectively equal to 71.02, 73.26, and 63.88). Next, for each set of observations, we implement posterior inference with truncated Gaussian series priors based on the Neumann–Laplacian eigenpairs and with the Matérn process prior, numerically computing the associated posterior mean estimates via the pCN algorithm. For the series priors, the regularity parameter in (18) is set to $\alpha = 3$. For the Matérn prior, the covariance hyperparameters in (16) are set to $\alpha = 3$ and $\ell = 0.25$. Across the three collections of experiments, the pCN algorithm is iterated for 25,000 steps, with a tuning of the step size to achieve a stabilisation of the acceptance rate between 20% and 30% after the burn-in (corresponding to the first 5000 samples). All the runs are initialised with cold starts. The obtained results are visualised in Figure 6 and summarised in Table 2. The computation times are in line with those of the experiments presented in Section 3.

B Proof of Theorem 1

We follow the proofs of Theorems 4–6 in [20], recalling two key properties of the forward operator G , holding for all $\alpha > 1 + d/2$,

$$\|G(\Phi \circ F_1) - G(\Phi \circ F_2)\|_{L^2} \lesssim (1 + \|F_1\|_{C^1}^4 + \|F_2\|_{C^1}^4) \|F_1 - F_2\|_{(H^1)^*}, \quad \forall F_1, F_2 \in H_0^\alpha(\mathcal{O}), \quad (21)$$

and

$$\sup_{F \in H_0^\alpha} \|G(\Phi \circ F)\|_{L^\infty} < \infty.$$

Step I: posterior contraction rates in prediction risk. We start with the derivation of the contraction rates in prediction risk (9). Set $\epsilon_n := n^{-(\alpha+1)/(2\alpha+2+d)}$. By an application of Theorem 13 and Lemmas 22 and 23 in [20], it is enough to show that for some sufficiently large constant $c_1 > 0$, there exists a constant $c_2 > 0$ such that

$$\Pi_n(F : \|G(\Phi \circ F) - G(\Phi \circ F_0)\|_{L^2} \leq c_1 \epsilon_n) \geq e^{-c_2 n \epsilon_n^2}, \quad (22)$$

and further that there exist measurable sets $\mathcal{W}_n \subseteq C^\beta(\mathcal{O})$ satisfying

$$\Pi_n(\mathcal{W}_n^c) \leq e^{-c_3 n \epsilon_n^2}; \quad \log N(\epsilon_n; \mathcal{W}_n, d_G) \lesssim n \epsilon_n^2, \quad (23)$$

for some $c_3 > 0$ large enough, where $d_G(F_1, F_2) := \|G(\Phi \circ F_1) - G(\Phi \circ F_2)\|_{L^2}$, and $N(\epsilon_n; \mathcal{W}_n, d_G)$ is the minimal number of balls of radius ϵ_n in the metric d_G needed to cover

\mathcal{A}_n .

The main difference compared to the proofs in [20] lies in the verification of the small ball probability estimate (22). We proceed lower bounding this quantity by, for sufficiently large $M > 0$,

$$\begin{aligned}\Pi_n(F : \|G(\Phi \circ F) - G(\Phi \circ F_0)\|_{L^2} \leq c_1 \epsilon_n, \|F - F_0\|_{C^1} \leq M) \\ \geq \Pi_n(F : \|F - F_0\|_{(H^1)^*} \leq k_1 \epsilon_n, \|F - F_0\|_{C^1} \leq M)\end{aligned}$$

for some $k_1 > 0$ (depending on c_1), having used (21). Recalling the assumption (8) on the approximating sequence $F_{0,n} \in \mathcal{H}_{W_n}$ and using (twice) the triangle inequality, the latter prior probability is greater than

$$\Pi_n(F : \|F - F_{0,n}\|_{(H^1)^*} \leq k_2 \epsilon_n, \|F - F_{0,n}\|_{C^1} \leq M') = \Pi_n(F : F - F_{0,n} \in B_1 \cap B_2)$$

for $k_2, M' > 0$, having defined $B_1 := \{F : \|F\|_{(H^1)^*} \leq k_2 \epsilon_n\}$ and $B_2 := \{F : \|F\|_{C^1} \leq M'\}$. The intersection $B_1 \cap B_2$ defines a symmetric set in the ambient Banach space $C^1(\mathcal{O})$; hence, recalling that, by linearity, the RKHS of the scaled Gaussian prior $\Pi_n(\cdot)$ coincides with the RKHS \mathcal{H}_{W_n} of the base prior $\Pi_{W_n}(\cdot)$, with the scaled RKHS norm being equal to $n^{d/(4\alpha+4+2d)} \|\cdot\|_{\mathcal{H}_{W_n}} = \sqrt{n} \epsilon_n \|\cdot\|_{\mathcal{H}_{W_n}}$ (e.g., Exercise 2.6.15 in [25]), an application of Corollary 2.6.18 in [25] gives the further lower bound

$$e^{-n\epsilon_n^2 \|F_{0,n}\|_{\mathcal{H}_{W_n}}^2} \Pi_n(B_1 \cap B_2) \geq e^{-k_3 n \epsilon_n^2} \Pi_n(B_1 \cap B_2),$$

for $k_3 > 0$ since $\|F_{0,n}\|_{\mathcal{H}_{W_n}} = O(1)$ by assumption. Now, B_1 and B_2 are closed, convex, and symmetric subsets of the ambient space $C^1(\mathcal{O})$, and therefore by the correlation inequality for Gaussian measures (cf. Lemma A.2 in [39]),

$$\Pi_n(B_1 \cap B_2) \geq \Pi_n(B_1) \Pi_n(B_2).$$

Recalling the definition of the scaled Gaussian priors $\Pi_n(\cdot)$ in (6), we have for $W \sim \Pi_{W_n}(\cdot)$,

$$\Pi_n(B_2) = \Pr(\|W\|_{C^1} \leq M' \sqrt{n} \epsilon_n) \geq \Pr(\|W\|_{C^1} \leq M'') > 0$$

for some $M'' > 0$ since $\sqrt{n} \epsilon_n > 1$ for all n . Lastly, recalling the continuous embedding $\mathcal{H}_{W_n} \subseteq H_0^\alpha(\mathcal{O})$ holding by assumption for some integer $\alpha > \beta + d/2$, $\beta \geq 1$, combining the metric entropy estimate

$$\begin{aligned}\log N(\eta; \{F \in \mathcal{H}_{W_n} : \|F\|_{\mathcal{H}_{W_n}} \leq 1\}, \|\cdot\|_{(H^1)^*}) \\ \leq \log N(\eta; \{F \in H_0^\alpha(\mathcal{O}) : \|F\|_{H^\alpha} \leq k_4\}, \|\cdot\|_{(H^1)^*}) \lesssim \eta^{-\frac{d}{\alpha+1}},\end{aligned}$$

cf. Lemma 19 in [26], with Theorem 1.2 in [40], yields

$$\Pi_n(B_1) = \Pr(\|W\|_{(H^1)^*} \leq k_2 \sqrt{n} \epsilon_n^2) \geq e^{-k_5 (\sqrt{n} \epsilon_n^2)^{-2} \frac{d}{d+1} (2 - \frac{d}{\alpha+1})^{-1}} = e^{-k_5 n \epsilon_n^2}.$$

The obtained estimates thus jointly conclude the verification of (22) for a large enough constant c_2 .

Next, for $K > 0$, define the sieves

$$\mathcal{W}_n := \{F : F = F_1 + F_2, \|F_1\|_{(H^1)^*} \leq K \epsilon_n, \|F_2\|_{\mathcal{H}_{W_n}} \leq M, \|F\|_{C^\beta} \leq M\}.$$

A direct application of Lemma 17 in [20] (with $\kappa = 1$ in their notation) gives that for any positive $Q > 0$, there exists sufficiently large K such that $\Pi_n(\mathcal{W}_n^c) \leq e^{-Qn\epsilon_n^2}$. We then take K that is large enough and argue as in the proof of Lemma 18 in [20] to deduce that $\log N(\epsilon_n; \mathcal{W}_n, d_G) \lesssim n\epsilon_n^2$. This concludes the verification of (23) and then also of the first claim (9) of Theorem 1 since by Theorem 13 in [20] we obtain that

$$\Pi_n \left(F \in \mathcal{W}_n : \|G(\Phi \circ F) - G(\Phi \circ F)\|_{L^2} \leq L\epsilon_n \middle| \{(Y_i, X_i)\}_{i=1}^n \right) = 1 - O_{P_{f_0}^{(n)}}(e^{-Dn\epsilon_n^2}) \quad (24)$$

as $n \rightarrow \infty$ for some $L, D > 0$.

Step II: remaining claims. Assume now that $\beta \geq 2$, and recall that $\alpha > \beta + d/2$ (with $\alpha, \beta \in \mathbb{N}$). Since $C^\beta(\mathcal{O}) \subset H^\beta(\mathcal{O})$, Lemmas 23 and 29 in [26] imply that for all $F \in \mathcal{W}_n$, with \mathcal{W}_n for the above sieve sets, we have $G(\Phi \circ F) \in H^{\beta+1}(\mathcal{O})$ and

$$\|G(\Phi \circ F)\|_{H^{\beta+1}} \lesssim 1 + \|\Phi \circ F\|_{H^\beta}^{\beta(\beta+1)} \lesssim 1,$$

with a multiplicative constant independent of F . Similarly, since $F_0 \in H_0^\alpha(\mathcal{O}) \subset H^\beta(\mathcal{O})$, $G(\Phi \circ F_0) \in H^{\beta+1}(\mathcal{O})$ and $\|G(\Phi \circ F_0)\|_{H^{\beta+1}} \lesssim 1$. By the standard interpolation inequality for Sobolev spaces, for all $F \in \mathcal{W}_n$, we then have

$$\begin{aligned} \|G(\Phi \circ F) - G(\Phi \circ F_0)\|_{H^2} &\lesssim \|G(\Phi \circ F) - G(\Phi \circ F_0)\|_{L^2}^{\frac{\beta-1}{\beta+1}} \|G(\Phi \circ F) - G(\Phi \circ F_0)\|_{H^\beta}^{\frac{2}{\beta+1}} \\ &\lesssim \|G(\Phi \circ F) - G(\Phi \circ F_0)\|_{L^2}^{\frac{\beta-1}{\beta+1}}. \end{aligned}$$

Combined with (24), this implies that

$$\Pi_n \left(F \in \mathcal{W}_n : \|G(\Phi \circ F) - G(\Phi \circ F_0)\|_{H^2} \leq L'\epsilon_n^{\frac{\beta-1}{\beta+1}} \middle| \{(Y_i, X_i)\}_{i=1}^n \right) = 1 - O_{P_{f_0}^{(n)}}(e^{-Dn\epsilon_n^2})$$

for $L' > 0$ as $n \rightarrow \infty$. The second claim (10) of Theorem 1 is then verified using the following stability estimate for the forward operator G ,

$$\|f_1 - f_2\|_{L^2} \lesssim \|f\|_{C^1} \|G(f) - G(f_0)\|_{H^2}$$

holding for all $f, f_0 \in \mathcal{F}_{\alpha, f_{\min}}$ (the parameter space from (5)) provided that $\alpha > 2+d/2$ and $\inf_{x \in \mathcal{O}} s(x) > 0$, cf. Lemma 24 in [26]. Indeed, combined with the second to last display, this gives

$$\Pi_n \left(F \in \mathcal{W}_n : \|\Phi \circ F - \Phi \circ F_0\|_{L^2} \leq L'\epsilon_n^{\frac{\beta-1}{\beta+1}} \middle| \{(Y_i, X_i)\}_{i=1}^n \right) = 1 - O_{P_{f_0}^{(n)}}(e^{-Dn\epsilon_n^2}).$$

Based on the last display, the proof of the last claim (11) now follows arguing exactly as for Theorem 6 in [20].

Acknowledgement. We are grateful to the Associate Editor and four anonymous referees for their helpful comments. This research has been partially supported by MUR, PRIN project 2022CLTYP4.

References

- [1] Engl, H.W.; Hanke, M.; Neubauer, A. *Regularization of Inverse Problems*; Mathematics and Its Applications; Kluwer Academic Publishers Group: Dordrecht, The Netherlands, 1996; Volume 375, p. viii+321.
- [2] Kaltenbacher, B.; Neubauer, A.; Scherzer, O. *Iterative Regularization Methods for Nonlinear Ill-Posed Problems*; Radon Series on Computational and Applied Mathematics; Walter de Gruyter GmbH & Co. KG: Berlin, Germany, 2008; Volume 6, p. viii+194. <https://doi.org/10.1515/9783110208276>.
- [3] Isakov, V. *Inverse Problems for Partial Differential Equations*, third ed.; Applied Mathematical Sciences; Springer: Cham, Switzerland, 2017; Volume 127, p. xv+406. <https://doi.org/10.1007/978-3-319-51658-5>.
- [4] Kaipio, J.; Somersalo, E. *Statistical and Computational Inverse Problems*; Number 160 in Applied Mathematical Sciences; Springer: New York, NY, USA, 2004.
- [5] Bissantz, N.; Hohage, T.; Munk, A. Consistency and rates of convergence of nonlinear Tikhonov regularization with random noise. *Inverse Probl.* **2004**, *20*, 1773–1789.
- [6] Hohage, T.; Pricop, M. Nonlinear Tikhonov regularization in Hilbert scales for inverse boundary value problems with random noise. *Inverse Probl. Imaging* **2008**, *2*, 271–290. <https://doi.org/10.3934/ipi.2008.2.271>.
- [7] Benning, M.; Burger, M. Modern regularization methods for inverse problems. *Acta Numer.* **2018**, *27*, 1–111. <https://doi.org/10.1017/S0962492918000016>.
- [8] Arridge, S.; Maass, P.; Öktem, O.; Schönlieb, C.B. Solving inverse problems using data-driven models. *Acta Numer.* **2019**, *28*, 1–174. <https://doi.org/10.1017/s0962492919000059>.
- [9] Nickl, R. *Bayesian Non-Linear Statistical Inverse Problems*; Zurich Lectures in Advanced Mathematics; EMS Press: Berlin, Germany, 2023; p. xi+159. <https://doi.org/10.4171/zlam/30>.
- [10] Evans, L.C. *Partial Differential Equations*, 2nd ed.; *Graduate Studies in Mathematics*; American Mathematical Society: Providence, RI, USA, 2010; Volume 19, p. xxii+749. <https://doi.org/10.1090/gsm/019>.
- [11] Yeh, W.W.G. Review of Parameter Identification Procedures in Groundwater Hydrology: The Inverse Problem. *Water Resour. Res.* **1986**, *22*, 95–108. <https://doi.org/10.1029/WR022i002p00095>.
- [12] Richter, G.R. An inverse problem for the steady state diffusion equation. *SIAM J. Appl. Math.* **1981**, *41*, 210–221. <https://doi.org/10.1137/0141016>.
- [13] Knowles, I. Parameter identification for elliptic problems. *J. Comput. Appl. Math.* **2001**, *131*, 175–194. [https://doi.org/https://doi.org/10.1016/S0377-0427\(00\)00275-2](https://doi.org/https://doi.org/10.1016/S0377-0427(00)00275-2).

- [14] Bonito, A.; Cohen, A.; DeVore, R.; Petrova, G.; Welper, G. Diffusion coefficients estimation for elliptic partial differential equations. *SIAM J. Math. Anal.* **2017**, *49*, 1570–1592. <https://doi.org/10.1137/16M1094476>.
- [15] Dashti, M.; Stuart, A.M. Uncertainty quantification and weak approximation of an elliptic inverse problem. *SIAM J. Numer. Anal.* **2011**, *49*, 2524–2542. <https://doi.org/10.1137/100814664>.
- [16] Cotter, S.; Roberts, G.; Stuart, A.; White, D. MCMC Methods for Functions: Modifying Old Algorithms to Make Them Faster. *Stat. Sci.* **2013**, *28*, 424–446.
- [17] Stuart, A.M. Inverse problems: A Bayesian perspective. *Acta Numer.* **2010**, *19*, 451–559.
- [18] Vollmer, S.J. Posterior consistency for Bayesian inverse problems through stability and regression results. *Inverse Probl.* **2013**, *29*, 125011. <https://doi.org/10.1088/0266-5611/29/12/125011>.
- [19] Abraham, K.; Nickl, R. On statistical Calderón problems. *Math. Stat. Learn.* **2019**, *2*, 165–216.
- [20] Giordano, M.; Nickl, R. Consistency of Bayesian inference with Gaussian process priors in an elliptic inverse problem. *Inverse Probl.* **2020**, *36*, 85001–85036.
- [21] Monard, F.; Nickl, R.; Paternain, G.P. Consistent inversion of noisy non-Abelian X-ray transforms. *Comm. Pure Appl. Math.* **2021**, *74*, 1045–1099. <https://doi.org/10.1002/cpa.21942>.
- [22] Giordano, M. Asymptotic Theory for Bayesian Nonparametric Inference in Statistical Models Arising from Partial Differential Equations. Doctoral Thesis, University of Cambridge, UK, 2021. <https://doi.org/10.17863/CAM.78120>.
- [23] Agapiou, S.; Wang, S. Laplace priors and spatial inhomogeneity in Bayesian inverse problems. *Bernoulli* **2024**, *30*, 878–910.
- [24] Ghosal, S.; van der Vaart, A.W. *Fundamentals of Nonparametric Bayesian Inference*; Cambridge University Press: New York, NY, USA, 2017.
- [25] Giné, E.; Nickl, R. *Mathematical Foundations of Infinite-Dimensional Statistical Models*; Cambridge University Press: New York, NY, USA, 2016; p. xiv+690. <https://doi.org/10.1017/CBO9781107337862>.
- [26] Nickl, R.; van de Geer, S.; Wang, S. Convergence rates for penalized least squares estimators in PDE constrained regression problems. *SIAM/ASA J. Uncertain. Quantif.* **2020**, *8*, 374–413. <https://doi.org/10.1137/18M1236137>.
- [27] Dashti, M.; Stuart, A.M. The Bayesian approach to inverse problems. In *Handbook of Uncertainty Quantification*; Springer: Cham, Switzerland, 2017; pp. 311–428.
- [28] Haroske, D.D.; Triebel, H. *Distributions, Sobolev Spaces, Elliptic Equations*; EMS Press, Berlin, Germany 2007.
- [29] Taylor, M.E. *Partial Differential Equations I*; Springer: New York, NY, USA, 2011.

- [30] Hairer, M.; Stuart, A.; Vollmer, S. Spectral Gaps for a Metropolis-Hastings Algorithm in Infinite Dimensions. *Ann. Appl. Probab.* **2014**, *24*, 2455–2490.
- [31] Hall, P.; Marron, J. On variance estimation in nonparametric regression. *Biometrika* **1990**, *77*, 415–419.
- [32] Wahba, G. Improper priors, spline smoothing and the problem of guarding against model errors in regression. *J. R. Stat. Soc. Ser. B Stat. Methodol.* **1978**, *40*, 364–372.
- [33] Rice, J. Bandwidth choice for nonparametric regression. *Ann. Statist.*; 1984, *12*, 1215–1230.
- [34] Kejzlar, V.; Son, M.; Bhattacharya, S.; Maiti, T. A fast and calibrated computer model emulator: An empirical Bayes approach. *Stat. Comput.* **2021**, *31*, 49.
- [35] Knapik, B.; Szabò, B.; van der Vaart, A.W.; van Zanten, H. Bayes procedures for adaptive inference in inverse problems for the white noise model. *Probab. Theory Relat. Fields* **2015**, *164*, 771–813.
- [36] Rousseau, J.; Szabo, B. Asymptotic behaviour of the empirical Bayes posteriors associated to maximum marginal likelihood estimator. *Ann. Stat.* **2017**, *45*, 833 – 865. <https://doi.org/10.1214/16-AOS1469>.
- [37] Teckentrup, A.L. Convergence of Gaussian process regression with estimated hyper-parameters and applications in Bayesian inverse problems. *SIAM/ASA J. Uncertain. Quantif.* **2020**, *8*, 1310–1337.
- [38] Agapiou, S.; Bardsley, J.M.; Papaspiliopoulos, O.; Stuart, A.M. Analysis of the Gibbs sampler for hierarchical inverse problems. *SIAM/ASA J. Uncertain. Quantif.* **2014**, *2*, 511–544.
- [39] Giordano, M.; Ray, K. Nonparametric Bayesian inference for reversible multidimensional diffusions. *Ann. Stat.* **2022**, *50*, 2872–2898.
- [40] Li, W.V.; Linde, W. Approximation, metric entropy and small ball estimates for Gaussian measures. *Ann. Probab.* **1999**, *27*, 1556–1578. <https://doi.org/10.1214/aop/1022677459>.